Intraband absorption in semiconductor quantum wells in the presence of a perpendicular magnetic field

S. Živanović, V. Milanović, and Z. Ikonić
Faculty of Electrical Engineering, University of Belgrade, Bulevar Revolucije 73, 11000 Belgrade, Yugoslavia
(Received 15 March 1995)

The intraband light absorption between conduction-band states in symmetric semiconductor quantum wells in the presence of a perpendicular magnetic field is discussed. By theoretical analysis three types of transitions are found: bound bound, bound free, and free free. Numerical calculations are given for a rectangular GaAs quantum well in bulk $Al_xGa_{1-x}As$. The absorption in this structure strongly depends on structure parameters (well thickness, mole fraction, and effective masses), and also on temperature and external magnetic field. Analysis and numerical results such as those presented here may be important for the design of infrared detectors.

I. INTRODUCTION

It is well known that in a semiconductor quantum well two types of optical transitions, interband and intraband, may occur. If the quantum-well structure is subjected to a magnetic field, these transitions become very interesting. The magnetic field is an important additional parameter, since it can be applied experimentally in a well-controlled way and modifies fundamentally the electronic structure. Interband transitions have been studied both theoretically and experimentally, giving considerable absorption of light with photon energies above the value of the energy gap[1,2] (for GaAs quantum well it is about 1.5 eV).

Three types of intraband transitions are allowed: bound bound, bound free, and free free (classified according to the nature of initial and final electron states). These transitions are significant for the photon energies of the order of tens or hundreds of meV, i.e., an order of magnitude lower than those inducing interband transitions.

In this paper we consider the intraband absorption in semiconductor quantum wells subjected to perpendicular magnetic field (Fig. 1). Parallel field has a small quantitative impact on the quantum well's energy spectrum and thus the absorption may also be expected to remain essentially unaffected.[3] If a field perpendicular to the quantum-well plane is applied, however, the energy spectrum is changed considerably, corresponding to the effective appearance of a large number of quantum wells displaced in energy according to the Landau-level index. This fact directly influences the nature of intraband transitions in these structures, as we discuss below.

II. ELECTRONIC STRUCTURE OF A QUANTUM WELL IN A PERPENDICULAR MAGNETIC FIELD

If a quantum well is placed in a perpendicular, spatially homogeneous and static magnetic field $\mathbf{B}\|\mathbf{e}_z$ (Fig. 1), the envelope function Schrödinger equation describing electron states in the structure reads

$$\hat{H}_0\Psi=\left[\tfrac{1}{2}(\hat{\mathbf{p}}+e\,\mathbf{A}_M)\frac{1}{m(z)}(\hat{\mathbf{p}}+e\,\mathbf{A}_M)+U(z)+sg^*(z)\mu_B B\right]\Psi=E\Psi\,, \tag{1}$$

where $\hat{H}_0$, E, and $\Psi(\mathbf{r})$ are the Hamiltonian, electron energy, and envelope function, while $U(z)$, $m(z)$, and $g^*(z)$ denote the spatially dependent potential (conduction-band edge), effective mass, and Landé g factor. The spin quantum number is s ($s=\pm\frac{1}{2}$), $\mu_B=e\hbar/2m_0$ is the Bohr magneton, and $\mathbf{A}_M$ is the magnetic vector potential. It was shown in Ref. 2 that spin splitting may be neglected because it is usually small; in GaAs, for instance, the effective Landé factor is $g^*=-0.445$, leading to a splitting $g^*\mu_B B$ of only 0.26 meV at 10 T.

It is well known that the magnetic vector potential $\mathbf{A}_M$ is not uniquely determined by the magnetic induction $\mathbf{B}$. The choice of gauge, however, has no effect on physical quantities such as electron concentration and absorption.

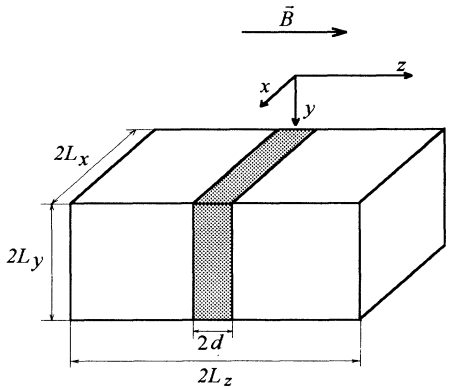

FIG. 1. Schematic representation of the quantum well in perpendicular magnetic field **B**. Dimensions of the full sample are $2L_x, 2L_y, 2L_z \to +\infty$.

We choose the vector potential as $\mathbf{A}_M=-By\mathbf{e}_x$, and the envelope wave functions may then be written in the product form

$$\Psi(x,y,z)=\frac{e^{ik_x x}}{\sqrt{2L_x}}\Phi_j(y-y_0)\eta(z)\ , \tag{2}$$

satisfying the normalization condition, where k_x is the x component of the wave vector, $\Phi_j(y-y_0)$ is the harmonic oscillator eigenfunction, with $y_0=\hbar k_x/eB$, and $\eta(z)$ is the solution of

$$-\frac{\hbar^2}{2}\frac{d}{dz}\left[\frac{1}{m(z)}\frac{d\eta(z)}{dz}\right]+\left[U(z)+\frac{eB\hbar}{m(z)}(j+\tfrac{1}{2})\right]\eta(z)=E\eta(z)\ . \tag{3}$$

If the electron effective mass is constant throughout the structure, $\eta(z)$ would be independent of the Landau index j, and the total electron energy would be the sum of $E_i(j=0)$ and $E_j=\hbar eB(j+\frac{1}{2})/m$, where E_i if the ith eigenenergy of Eq. (3). In other words, the Schrödinger equation (3) might then be solved for just a single value of j, $j=0$, say. However, with variable $m(z)$, as it is in reality, Eq. (3) has to be solved separately for each j value, the wave function $\eta_{i,j}(z)$ becomes dependent on j, and the total energy $E_{i,j}$ is no more representable as a sum of two separate terms.

III. THE INTERACTION HAMILTONIAN AND TRANSITION-MATRIX ELEMENTS

Consider a monochromatic light wave, characterized by the magnetic vector potential $\mathbf{A}_R=A_R\mathbf{a}_r$ ($|\mathbf{a}_r|=1$), incident on a quantum well. The electromagnetic field of input light represents the perturbation, which can cause the absorption of light. We will analyze the general case when all three components of the vector $\mathbf{A}_R$ are nonzero. The polarization unit vector $\mathbf{a}_r$ has components $\cos\varphi\sin\theta$, $\sin\varphi\sin\theta$, and $\cos\theta$, where θ is the angle between $\mathbf{A}_R$ and the z axis, and φ is the angle between the x axis and x-y projection of $\mathbf{A}_R$.

If the well is subjected to both the static magnetic field and the light wave, then $\mathbf{A}_M$ in the Schrödinger equation is replaced with $\mathbf{A}_M+\mathbf{A}_R$. Denoting the Hamiltonian with both $\mathbf{A}_M$ and $\mathbf{A}_R$ by $\hat{H}$, the interaction Hamiltonian is $\hat{H}'=\hat{H}-\hat{H}_0$. We can choose the gauge such that the vector potential satisfies $\operatorname{div}\mathbf{A}_R=0$. The interaction Hamiltonian then has the form

$$\hat{H}'=e\,\mathbf{A}_R\left[\frac{1}{m}\hat{\mathbf{p}}+\frac{1}{2}\hat{\mathbf{p}}\frac{1}{m}+\frac{e}{2m}(\mathbf{A}_R+2\mathbf{A}_M)\right]\ . \tag{4}$$

The velocity operator for the nonilluminated system is

$$\hat{\mathbf{v}}_0=\frac{i}{\hbar}[\hat{H}_0,\hat{\mathbf{r}}]=\frac{i}{\hbar}(\hat{H}_0\hat{\mathbf{r}}-\hat{\mathbf{r}}\hat{H}_0)=\frac{1}{m}\hat{\mathbf{p}}+\frac{1}{2}\hat{\mathbf{p}}\frac{1}{m}+\frac{e\,\mathbf{A}_M}{m}\ . \tag{5}$$

Now, we can rewrite the interaction Hamiltonian using Eq. (5) and neglecting the term proportional to $\mathbf{A}_R^2$.

$$\hat{H}'=\hat{H}-\hat{H}_0=e\,\mathbf{A}_R\left[\hat{\mathbf{v}}_0+\frac{e}{2m}\mathbf{A}_R\right]\approx e\,\mathbf{A}_R\hat{\mathbf{v}}_0\ . \tag{6}$$

The use of the velocity operator is appropriate, because the effective mass is the function of the coordinate z. From the relation defining the transition-matrix element P_{if} we have

$$P_{if}=\int_\Omega\Psi_i^*\hat{H}'\Psi_f d^3r=eA_R\int_\Omega\Psi_i^*\mathbf{a}_r\hat{\mathbf{v}}_0\Psi_f d^3r\ . \tag{7}$$

Due to the position dependence of the effective mass the potential appearing in $\hat{H}$ and $\hat{H}_0$ is nonlocal,[4] the velocity cannot be written as $[\hat{\mathbf{p}}+e(\mathbf{A}_M+\mathbf{A}_R)]/m$, and the expression (7) for P_{if} is the only possible form. To calculate the transition-matrix element $P_{if}\equiv e\,\mathbf{A}_R\cdot\mathbf{M}_{if}$, we use Eq. (2) for the wave function, and with $\mathbf{A}_M=-By\mathbf{e}_x$ we find that components of $\mathbf{M}_{if}$ are

$$M_{ifx}=iM_{ify}=-\sqrt{eB\hbar}\left[\frac{j_i+1}{2}\right]^{1/2}\int_{-\infty}^{+\infty}\frac{\eta_{i_i,j_i}^*\eta_{i_f,j_f}}{m(z)}dz\ ,\quad j_f=j_i+1,\quad k_{ix}=k_{fx}\ , \tag{8}$$

$$M_{ifx}=-iM_{ify}=-\sqrt{eB\hbar}\left[\frac{j_i}{2}\right]^{1/2}\int_{-\infty}^{+\infty}\frac{\eta_{i_i,j_i}^*\eta_{i_f,j_f}}{m(z)}dz\ ,\quad j_f=j_i-1,\quad k_{ix}=k_{fx}\ , \tag{9}$$

$$M_{ifz}=-i\hbar\left[\int_{-\infty}^{+\infty}\frac{\eta_{i_i,j_i}^*}{m}\frac{d\eta_{i_f,j_f}}{dz}dz+\tfrac{1}{2}\int_{-\infty}^{+\infty}\eta_{i_i,j_i}^*\eta_{i_f,j_f}\frac{d}{dz}\frac{1}{m}dz\right]\ ,\quad j_f=j_i,\quad k_{ix}=k_{fx}\ , \tag{10}$$

where j_i and j_f are quantum numbers of the initial and final state, respectively. One should notice that M_{ifx} and M_{ify} are zero if the electron effective mass is independent of z, while M_{ifz} in that case is nonzero for $j_f=j_i$. Also, M_{ifx} and M_{ify} are nonzero only for transitions where quantum number j changes by 1, while M_{ifx} is nonzero for $j_f=j_i$. Of course, the x component of the wave vector must be conserved ($k_{ix}=k_{fx}$). Since the quantum well is symmetric, i.e., $U(z)$ and $m(z)$ are even functions, from Eqs. (8)–(10) we can conclude that for the $j_i=j_f$ transitions the initial and final wave functions should have opposite parity, otherwise they should have the same parity. Finally,

$$|P_{if}|^2=\begin{cases}M_{ifx}^2\sin^2\theta e^2A_R^2, & j_f=j_i+1\vee j_f=j_i-1\ ,\\ M_{ifz}^2\cos^2\theta e^2A_R^2, & j_f=j_i\ .\end{cases} \tag{11}$$

One should notice that for the $j_f=j_i-1$ transitions Eq. (9) is similar to Eq. (8) for the $j_f=j_i+1$ transitions, provided j_i+1 in Eq. (8) is replaced by j_i.

IV. INTRABAND ABSORPTION

We first discuss transitions between two bound states with energies E_i and E_f. The absorption coefficient in this case is given by[2]

$$\alpha=\frac{\pi}{Vn\varepsilon_0 c\omega}|P_{if}|^2\delta(E_f-E_i-\hbar\omega)\phi_{if} ,$$
$$\phi_{if}=\frac{1}{e^{(E_i-E_F)/kT}+1}-\frac{1}{e^{(E_f-E_F)/kT}+1} , \tag{12}$$

where $V=2L_z2L_x2L_y$ is the sample volume, ϕ_{if} is the difference between the Fermi-Dirac functions of final and initial states, and $\hbar\omega$ is the photon energy. This expression holds for any specified k_x value. However, states with different k_x are degenerate, and, proceeding in the usual way, we find that the fractional absorption $A_{if}=2L_z\alpha$ is

$$A_{if}=\frac{2\pi\beta eB}{n\omega}|P_{if}^*|^2\delta(E_f-E_i-\hbar\omega)\phi_{if} ,$$
$$\beta=\frac{1}{4\pi}\frac{e^2}{\hbar\varepsilon_0 c}\approx\frac{1}{137}, \quad P_{if}^*=\frac{P_{if}}{eA_R} . \tag{13}$$

Within bound-bound transitions there exist three types: $j_i=j_f$, $j_f=j_i-1$, and $j_f=j_i+1$.

The absorption for bound-free transitions is found by integrating Eq. (13) over all k_z values, $k_z\in(0,+\infty)$:

$$A_{if}=\frac{2\beta eB}{n\omega}\frac{m_b}{\hbar^2k_{zf0}}|L_zP_{ij}^*(k_{zf0})|^2\phi_{if}(E_i+\hbar\omega,E_i) ,$$
$$E_f(k_{zf0})=E_i+\hbar\omega , \tag{14}$$

where

$$k_{zf0}=\left[\frac{2m_b}{\hbar^2}[E_i+\hbar\omega-\hbar\omega_c(j_f+\tfrac{1}{2})]\right]^{1/2} ,$$
$$\omega_c=\frac{\hbar eB}{m_b} . \tag{15}$$

Within bound-free transitions there also exist three types: $j_i=j_f$, $j_f=j_i-1$, and $j_f=j_i+1$. In Eqs. (14) and (15) m_b is the bulk (barrier) effective mass.

To obtain the absorption for free-free transitions, we must integrate Eq. (13) over the z component of the wave vector of both initial and final states:

$$A_{if}=\frac{2\beta eB}{n\pi\omega}\int_0^{+\infty}|L_zP_{if}^*(k_{zf0},k_{zi})|^2 \times\phi_{if}(E_f(k_{zf0}),E_i(k_{zi}))\frac{m_b}{\hbar^2k_{zf0}}dk_{zi} , \tag{16}$$

where

$$E_f(k_{zf0})=E_i(k_{zi})+\hbar\omega ,$$
$$k_{zf0}=\left[k_{zi}^2+\frac{2\omega m_b}{\hbar}\right]^{1/2} . \tag{17}$$

For free-free $j_f=j_i+1$ transitions, it can be shown that the absorption coefficient is equal to the absorption coefficient of barrier material. The presence of the quantum well contributes to the additional fractional absorption, the analysis of which will be given in another paper. Free-free transitions with $j_f=j_i-1$ turn out to be forbidden.

V. THE CASE OF THE RECTANGULAR QUANTUM WELL

We apply the above theory to the case of the rectangular quantum well [$U(z)=-U_0$ in the well and $U(z)=0$ in the barrier (Fig. 2)]. The effective mass here is piecewise constant, being m_w in the well and m_b in the barrier. In a homogeneous magnetic field **B** the effective potential in the Schrödinger equation (3) is $U_{\text{eff}}(z)=U(z)+eB\hbar(j+\frac{1}{2})/m(z)$ (Fig. 3). Due to the spatially dependent effective mass ($m_w<m_b$), the conduction-band edge will be raised more in the well then in the barrier resulting in the restriction for the Landau index j. Thus, j can take values between zero and $j_{\max}$ for which the potential profile is still of the quantum well, not barrier, type.

In accordance with the symmetry of the quantum well, the wave functions are either even or odd. Applying the continuity of the wave function and of

$$\frac{1}{m_w}\frac{d\eta_w(z)}{dz}\bigg|_{z=d^-}=\frac{1}{m_b}\frac{d\eta_b(z)}{dz}\bigg|_{z=d^+} , \tag{18}$$

we get transcendental equations for the discrete energy spectrum of electrons in the quantum well in the magnetic field. Even states:

$$\tan kd=\frac{k'}{k}\frac{m_w}{m_b} ,$$

odd states:

$$\tan kd=-\frac{k}{k'}\frac{m_b}{m_w} , \tag{19}$$

where k and k' are the z components of the wave vector in the well and barrier, respectively. The electron wave functions $\eta(z)$ for discrete energy states are as follows.

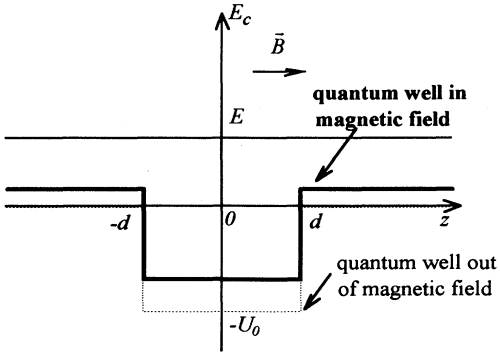

FIG. 2. The potential structure of the quantum well in and out of the magnetic field.

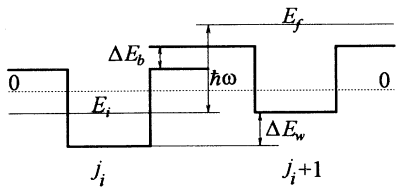

$$\Delta E_b = \frac{eB\hbar}{m_b}$$
$$\Delta E_w = \frac{eB\hbar}{m_w}$$

FIG. 3. Transition between discrete energy level E_i and continuous energy level E_f ($j_f = j_i + 1$).

$$\eta_e(z) = \begin{cases} A_e \cos kz, & |z| \le d \\ A_e \cos kd\, e^{-k'(z-d)}, & |z| > d \end{cases},$$
$$A_e = \frac{1}{\sqrt{d}} \frac{1}{\sqrt{1+\sin(2kd)/2kd + \cos^2(kd)/k'd}}, \tag{20}$$

for the even solution,

$$\eta_o(z) = \begin{cases} A_o \sin kz, & |z| \le d \\ A_o \sin kd\, e^{-k'(z-d)}, & |z| > d \end{cases},$$
$$A_o = \frac{1}{\sqrt{d}} \frac{1}{\sqrt{1-\sin(2kd)/2kd + \sin^2(kd)/k'd}}, \tag{21}$$

for the odd solution,

$$k(E) = \left[\frac{2m_w}{\hbar^2} \left[U_0 + E - \frac{eB\hbar}{m_w}(j+\tfrac{1}{2}) \right] \right]^{1/2},$$
$$k'(E) = \left[\frac{2m_b}{\hbar^2} \left[-E + \frac{eB\hbar}{m_b}(j+\tfrac{1}{2}) \right] \right]^{1/2}. \tag{22}$$

If the electron energy exceeds the barrier height (Fig. 2), i.e., $E > eB\hbar(j+\frac{1}{2})/m_b$, we deal with the continuous part of energy spectrum. The wave functions $\eta(z)$ of these states may also be even wave functions:

$$\eta_{w,e}(z) = \begin{cases} A_{ec} \cos(kz)/\sqrt{L_z}, & |z| \le d \\ \cos(k'z + \varphi_e)/\sqrt{L_z}, & |z| > d', \end{cases}$$
$$A_{ec}^2 = \frac{1+\tan^2(kd)}{1+[(k/k')m_b/m_w \tan(kd)]^2}, \tag{23}$$
$$\varphi_e = \arctan\left[\frac{k}{k'} \frac{m_b}{m_w} \tan(kd) \right] - k'd,$$

or odd wave functions:

$$\eta_{w,o}(z) = \begin{cases} A_{oc} \sin(kz)/\sqrt{L_z}, & |z| \le d \\ \sin(k'z + \varphi_0)/\sqrt{L_z}, & |z| > d, \end{cases}$$
$$A_{oc}^2 = \frac{[(k/k')m_b/m_w)]^2[1+\tan^2(kd)]}{1+[k/k'm_b/m_w \tan(kd)]^2}, \tag{24}$$
$$\varphi_o = \arctan\left[\frac{k'}{k} \frac{m_w}{m_b} \tan(kd) \right] - k'd,$$

where $k(E)$ have the same form as in Eq. (2), while $[k'(E)]^2 = [E - (eB\hbar/m_b)(j+\frac{1}{2})]2m_b/\hbar^2$. From the boundary condition at $z = d$, we get the following equation for the even solution, say

$$km_b \tan(kd) = k'm_w \tan(k'd + \varphi_e) \tag{25}$$

from which the phase φ_e may be found to within an integer multiple of π. This in turn may be found from Levinson's theorem,[5] but it is not necessary if the transition-matrix element squared is the quantity of interest; Eq. (25) alone is enough for this purpose.

We proceed with the expressions for matrix elements in the case of the rectangular quantum well. First, for bound-bound transitions ($j_f = j_i$), the component M_{ifz}^* for the even initial state and the odd final state reads

$$M_{ifz}^* = -M_{ifz}/i\hbar = \frac{A_{ei} A_{of} k_f}{m_w} \left[\frac{\sin(k_i + k_f)d}{k_i + k_f} + \frac{\sin(k_i - k_f)d}{k_i - k_f} \right]$$
$$- \frac{2A_{ei} A_{of} k_f'}{m_b(k_i' + k_f')} \cos k_i d \sin k_f d + A_{ei} A_{of} \left[\frac{1}{m_b} - \frac{1}{m_w} \right] \cos k_i d \sin k_f d. \tag{26}$$

The corresponding expression for the other possibility (odd initial state and even final state) is similar to Eq. (26). In the case of bound-bound transitions ($j_f = j_i + 1$), only M_{ifx} and M_{ify} are nonzero [Eq. (8)]. If the wave functions of both the initial and final states are even, M_{ifx} is given by

$$M_{ifx} = -\sqrt{eB\hbar} \left[\frac{j_i+1}{2} \right]^{1/2} \left\{ \frac{A_{ei} A_{ef}}{m_w} \left[\frac{\sin(k_i + k_f)d}{k_i + k_f} + \frac{\sin(k_i - k_f)d}{k_i - k_f} \right] + \frac{2A_{ei} A_{ef}}{m_b(k_i' + k_f')} \cos k_i d \cos k_f d \right\}. \tag{27}$$

When the initial and final wave functions are both odd, the expression for M_{ifx} can be obtained analogously. Finally, for bound-bound transitions with $j_f = j_i - 1$ Eq. (27) also applies upon the substitution of $j_i + 1$ by j_i.

For bound-free $j_f = j_i$ transitions, in the case of even initial state and odd final state, we have

$$\sqrt{L_z}M^*_{ifz}=\frac{A_{ei}A_{ocf}k_f}{m_w}\left[\frac{\sin(k_i+k_f)d}{k_i+k_f}+\frac{\sin(k_{i1}-k_f)d}{k_i-k_f}\right]$$
$$+\frac{2A_{ei}k'_f}{m_b}\frac{\cos k_i d}{k_i'^2+k_f'^2}[k'_i\cos(k'_f d+\varphi_{of})-k'_f\sin(k'_f d+\varphi_{of})]+A_{ei}A_{ocf}\left[\frac{1}{m_b}-\frac{1}{m_w}\right]\cos k_i d\sin k_f d\ . \quad (28)$$

For bound-free $j_f=j_i+1$ transitions (Fig. 3), as derived above, M_{ifx} and M_{ify} are nonzero [Eq. (8)]. For the sake of simplicity, we write k'_f instead of k_{zf0} in Eqs. (14) and (15). If the wave functions of the initial and final state are both even, we find

$$\sqrt{L_z}M_{ifx}=-\sqrt{eB\hbar}\left[\frac{j_i+1}{2}\right]^{1/2}\left\{\frac{A_{ei}A_{ecf}}{m_w}\left[\frac{\sin(k_i+k_f)d}{k_i+k_f}+\frac{\sin(k_i-k_f)d}{k_i-k_f}\right]\right.$$
$$\left.+\frac{2A_{ei}}{m_b}\frac{\cos k_i d}{k_i'^2+k_f'^2}[k'_i\cos(k'_f d+\varphi_{ef})-k'_f\sin(k'_f d+\varphi_{ef})]\right\}, \quad (29)$$

while the case of odd initial and final states is solved similarly.

For bound-free transitions ($j_f=j_i-1$) the same equations can be used upon substitution of j_i+1 by j_i. Within this kind of transition we distinguish two different possibilities depending on the position of the initial energy E_i with respect to the effective barrier level of the final state. If the discrete energy level E_i satisfies $E_i<\hbar\omega_c(j_i-1+\frac{1}{2})$, i.e., E_i is below the j_i-1 barrier level, then the only possible transitions are those from initial bound state to final free state with $j_f=j_i-1$ [Fig. 4(a)], if the photon energy is large enough.

The energy structure for $E_i>\hbar\omega_c(j_i-1+\frac{1}{2})$ is shown at Fig. 4(b). This is a particularly interesting situation, because two different types of transitions are recognized: (1) The transitions from the initial bound state (j_i) to the final free state (j_i-1) are allowed for all photon energies. (2) The transition from an initial free state (j_i-1) to the final bound state (j_i) is possible in a restricted range of photon energies. This is a type of optical transition that, to our knowledge, does not appear in other quantum systems.

VI. NUMERICAL RESULTS AND DISCUSSION

The bound-state energies are determined by the well width, Al mole fraction x in the $Al_xGa_{1-x}As$ barrier (with the corresponding values of the electron effective mass and the well depth), and the magnetic field B. With increasing Landau index j the overall effective potential in the structure gets higher, and so do the total energies of bound states. There is an additional effect: due to the difference of the well and barrier effective masses, the one in GaAs being lower makes the well bottom increase faster than the barrier top. The well therefore becomes more and more shallow as j increases, setting a maximum value of j ($j_{\max}$) that bound states may acquire.

Numerical calculations were performed for GaAs quantum wells in the $Al_xGa_{1-x}As$ bulk. The electron effective mass dependence on the Al mole fraction x is taken as $m_b=(0.067+0.083x)m_0$ and the refractive index as $n=(3.6-0.7)x$, after Ref. 6. The conduction-band edge discontinuity at the $GaAs/Al_xGa_{1-x}As$ interface, i.e., the well depth, is given by $U_0=0.65\times1.247x$ [eV].

The structure with the quantum well is taken to be uniformly doped, so that the doping level determines the Fermi level E_F, which in turn establishes electron distribution over the available quantum states. The value of E_F is found from the transcendental equation

$$N_d=\sum_{j=0}^{+\infty}n_j=\frac{eB}{\pi^2\hbar^2}\sqrt{2m_bkT}\sum_{j=0}^{+\infty}\frac{dF_{1/2}(\eta_j)}{d\eta_j}\ ,$$
$$\eta_j=\frac{E_F-E_j}{kT}\ , \quad (30)$$

where N_d is the donor-type impurity concentration and $F_{1/2}$ the Fermi integral.

The Fermi level, found from Eq. (30), depends not only on doping and temperature, but on the magnetic field B as well. It increases with increasing B, although this is not very pronounced for $B\leq20$ T.

In calculating the absorption we introduce the phenomenological transition linewidth Γ by replacing the Dirac δ function by a Lorentzian[7]

$$\delta(E_f-E_i-\hbar\omega)\approx\frac{1}{\pi\Gamma}\frac{1}{1+[(E_f-E_i-\hbar\omega)/\Gamma]^2}\ , \quad (31)$$

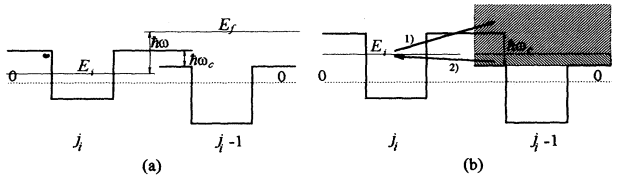

FIG. 4. Bound-free transitions $j_f=j_i-1$: (a) Energy level E_i is below the barrier level (j_i-1); energy level E_i is above the barrier level (j_i-1) and initial-free-to-final-bound transitions are possible too.

$$\Gamma=\left[\frac{2}{\pi}\right]^{1/2}\frac{\hbar e}{m^*}\left[\frac{B}{\mu}\right]^{1/2},$$
$$\mu=0.8\left[\frac{300}{T[\mathrm{K}]}\right]^{2.3}\left[\frac{m^2V}{s}\right],\quad m^*=0.067m_0\ . \tag{32}$$

The results of numerical calculations are presented in Fig. 5, where the absorption versus photon energy dependences for both x and z polarization are shown. In case of z polarization the absorption stems from transitions with the Landau index conserved, $j_f=j_i$, while in case of x polarization the transitions with $j_f=j_i\pm1$ both contribute. However, in the specific cases studied here, the transitions with $j_i=j_f+1$ give a negligible contribution. Also, among the bound-free transitions, those with $j_i=j_f$ are comparatively unimportant, the absorption on them never exceeding 1%.

The bound-free absorption has maximum photon energies ($\sim$150 meV) not very much exceeding the threshold ("ionization") value, which steadily decrease afterwards. The linewidth of these transitions is much larger then for bound-bound ones. Transitions with $j_f=j_i+1$ are found to give very low absorption.

As one can see from Fig. 5, the absorption maxima for x-polarized light exceed those for z-polarized light, although the absorption arising on transitions between individual pairs of states is larger for the case of z polarization. This is because photon energies corresponding to absorption maxima are well away from each other for z polarization, and quite close for x polarization. Therefore, when contributions of all the transitions are added together, this results in a higher, but more narrow, peak of total absorption for the x polarization. At elevated temperatures [$\sim$300 K, Fig. 5(b)] the absorption of the z-polarized light acquires additional peaks, due to increased population of higher levels. In not very wide wells, e.g., $2d=10$ nm [Fig. 5(b)], these peaks are quite distinct, but in wide ones ($2d=25$ nm) they tend to merge, making it difficult to tell one from another (as the well width increases the intensities of individual peaks become about equal). It is interesting to note that the absorption of x-polarized (e.g., normally incident) light gets smaller as the magnetic field decreases. However, even at $B=0$ there remains a small residual absorption which, in the case of symmetric structures, appears only on even-even and odd-odd transitions, and is due to the z-dependent effective-mass–induced coupling of electron motion in the x-y plane to the z coordinate. This effect has been predicted in a couple of papers,[8–10] using various approaches (all of them taking $B=0$ throughout the derivation). It can also be obtained, in a somewhat more difficult manner, by considering the limit $B\to0$ in Eq. (9). Calculations[10] of this type of absorption indicate that rather small values ($\sim$0.1% at peak) may be expected in real structures. This is very much smaller than what one gets in p-doped wells, or in n-doped wells in higher fields (Fig. 5), and is a probable reason that, to our knowledge, there lacks any experimental confirmation of absorption at normal incidence for $B=0$. At larger fields, however, the wave functions in Eq. (9) correspond to "different"

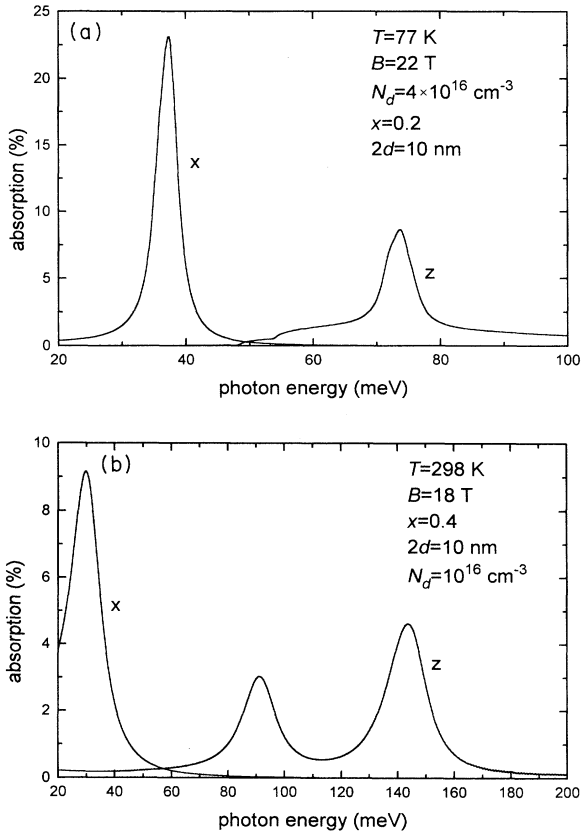

FIG. 5. The fractional absorption vs the photon energy dependence for a GaAs QW embedded in $Al_xGa_{1-x}As$ bulk, in a perpendicular magnetic field B.

wells due to the quantum number j nonconservation, as discussed above, and are therefore less orthogonal, resulting in the enhancement of normal incidence absorption.

Free-free transitions play only a minor role in the total absorption. Their intensity generally decreases as the photon energy increases, with no pronounced peaks.

Generally, the absorption profiles of quantum wells in the magnetic field considerably depend on the structure parameters (well width, doping level, temperature, magnetic field). The sensitivity to all these is more pronounced than in the zero magnetic field case, which is due to a more complex energy spectrum when a finite magnetic field is present.

The cyclotron resonance may be important for photon energies close to $\hbar\omega_c$, e.g., in the range 1.15–23 meV for $B=1$–20 T, which is out of the interval where transitions between quantized states in the structures considered here occur.

VII. CONCLUSION

Intraband transitions between quantized states of a semiconductor quantum well in a perpendicular magnetic field are analyzed and classified. Numerical calculation of absorption arising on various transitions was performed, and those giving the largest contributions indicated.

[1]H. Chu and Y. C. Chang, Phys. Rev. B **40**, 5497 (1989).
[2]U. Bockelmann and G. Bastard, Phys. Rev. B **45**, 1700 (1992).
[3]B. Mitrović, V. Milanović, and Z. Ikonić, Semicond. Sci. Technol. **6**, 93 (1991).
[4]E. De Salvo, R. Girlanda, and A. Quattropani, Nuovo Cimento **5D**, 63 (1985).
[5]V. Milanović, Z. Ikonić, and D. Tjapkin, Phys. Lett. A **170**, 127 (1992).
[6]S. Adachi, J. Appl. Phys. **R1**, 58 (1985).
[7]T. Ando, A. B. Fowler, and F. Stern, Rev. Mod. Phys. **54**, 637 (1982).
[8]A. G. Petrov and A. Shik, Phys. Rev. B **48**, 11 883 (1993).
[9]R. Q. Yang, J. M. Xu, and M. Sweeny, Phys. Rev. B **50**, 7474 (1994).
[10]Z. Ikonić and V. Milanović, in *Quantum Well Intersubband Transition Physics and Devices,* edited by H. C. Liu *et al.* (Kluwer Academic, Dordrecht, 1994), p. 389.